

Role of oxygen on chemical segregation in uncapped $\text{Ge}_2\text{Sb}_2\text{Te}_5$ thin films on silicon nitride

Shalini Tripathi¹, Paul Kotula², Manish Singh¹, Chanchal Ghosh¹, Gokhan Bakan³,
Helena Silva¹, C. Barry Carter^{4,5}

¹Electrical & Computer Engineering, University of Connecticut, Storrs, CT 06269

²Materials Science & Engineering Center, Sandia National Lab, Albuquerque, NM 87123

³The National Graphene Institute, University of Manchester, Manchester, M13 9PL, UK

⁴Chemical & Biomolecular Engineering, University of Connecticut, Storrs, CT 06269

⁵Center for Integrated Nanotechnologies (CINT), Sandia National Lab, Albuquerque, NM 87123

Abstract

Germanium antimony telluride has been the most used and studied phase-change material for electronic memory due to its suitable crystallization temperature, amorphous to crystalline resistance contrast, and stability of the amorphous phase. In this work, the segregation of Ge in a $\text{Ge}_2\text{Sb}_2\text{Te}_5$ film of 30 nm thickness during heating inside the transmission electron microscope was observed and characterized. The $\text{Ge}_2\text{Sb}_2\text{Te}_5$ film was deposited using sputtering on a Protochips Fusion holder and left uncapped in atmosphere for about four months. Oxygen incorporated within the film played a significant role in the chemical segregation observed which resulted in amorphous Ge-O island boundaries and Sb and Te rich crystalline domains. Such composition changes can occur when the phase-change material interfaces insulating oxide layers in an integrated device and can significantly impact its electrical and thermal properties.

Phase-change memory (PCM) is a new technology for non-volatile electronic memory, significantly faster than flash memory¹⁻³. Extensive work on the crystallization and amorphization properties of phase-change materials has been carried out to clarify the functional physical properties of suitable materials and explore their phase transformation dynamics. In addition to the phase transformation, chemical segregation and oxidation of the material are important issues that must be understood for proper integration of PCM devices. The most promising and commonly used material for PCM has been $\text{Ge}_2\text{Sb}_2\text{Te}_5$, which can exist in metastable amorphous or crystalline *fcc* phases, or in the stable crystalline *hexagonal* phase⁴⁻⁶. Numerous studies have focused on characterization of its electrical resistivity and functional behavior⁷⁻⁹ and some also on its microscopic and microchemical nature¹⁰.

It has been shown that $\text{Ge}_2\text{Sb}_2\text{Te}_5$ is prone to oxidation, especially formation of germanium oxide, and that the surface layers of a $\text{Ge}_2\text{Sb}_2\text{Te}_5$ thin film exposed to oxygen become depleted of Te and transform into Ge-O and Sb-O¹¹. Phase segregation also takes place at the interface between the GST and electrodes, limiting device endurance¹². It has been observed in endurance tests of $\text{Ge}_2\text{Sb}_2\text{Te}_5$ devices that Ge segregates towards material interfaces and can oxidize there¹³. Studies on oxygen-incorporated $\text{Ge}_2\text{Sb}_2\text{Te}_5$ films showed an increase in the amorphous-fcc phase transition and formation of non-stoichiometric GeO and phase separation into Sb_2O_3 and Sb_2Te_3 ¹⁴.

Oxidation of the $\text{Ge}_2\text{Sb}_2\text{Te}_5$ films always has an effect on the phase transformation behavior and the reaction kinetics with thermal treatment¹⁵⁻¹⁷, mainly due to compositional changes on a localized scale¹⁸⁻¹⁹. However, imaging and quantification of the chemical changes due to oxidation have been mainly deliberated as average thin film properties. The role of oxygen on the crystallization and chemical segregation in different morphology $\text{Ge}_2\text{Sb}_2\text{Te}_5$ materials at localized scales is not yet well understood¹⁸⁻²⁰ and microscopic evidence is still limited.

Kooi and coworkers¹⁹ have reported that oxidation of $\text{Ge}_2\text{Sb}_2\text{Te}_5$ significantly affects its crystallization temperature. They showed through in-situ transmission electron microscopy (TEM) studies that a 10 nm film kept in ambient condition for 2 weeks required only 35°C for complete transformation from amorphous to crystalline phase whereas films kept in vacuum required 130°C. They also observed amorphous grain boundaries in the crystalline phase, likely due to formation of amorphous germanium oxide. Of the elements present in the $\text{Ge}_2\text{Sb}_2\text{Te}_5$, Ge is more prone to oxidation owing to its affinity towards oxygen, leading to preferential oxidation of Ge. The remaining film is then rich in Sb and Te. A systematic and quantitative study of chemical changes

at varying temperatures preferably at atomic scale is required to unearth issues related to chemical segregation and phase separations in $\text{Ge}_2\text{Sb}_2\text{Te}_5$ with oxygen incorporated. Agati and coworkers have studied the effect of impurity inclusions on the nature of crystallization in Ge-rich $\text{Ge}_2\text{Sb}_2\text{Te}_5$ thin films. The presence of O and N was found to promote nucleation due to the abundance of heterogeneous nucleation sites²⁰⁻²¹. Berthier and coworkers observed that oxidation in GeTe phase-change thin films promotes crystallization and demonstrated that a SiN capping layer increased the crystallization temperature substantially²².

In this work we perform a systematic microscopic investigation to map and quantify the chemical changes and the compositional segregation in uncapped Ge-rich $\text{Ge}_2\text{Sb}_2\text{Te}_5$ films exposed to atmosphere, as a function of temperature.

$\text{Ge}_2\text{Sb}_2\text{Te}_5$ thin films were deposited over amorphous SiN_x in Protochips holders by 20 W (DC) power sputtering using a $\text{Ge}_2\text{Sb}_2\text{Te}_5$ target, in 10 mTorr with 10 sccm Ar. The GST films were left uncapped and kept in atmosphere. Protochips holders (Aduro 300) were used for in-situ heating of the $\text{Ge}_2\text{Sb}_2\text{Te}_5$ film inside the TEM. The target thickness of the deposited film was 30 nm. Deposited and target thicknesses were found to be in close agreement through Electron energy-loss spectroscopy (EELS) measurements which yielded a 38 nm SiN membrane thickness, compared to ~ 40 nm specified by the holder manufacturer.

Microstructural and microchemical characterization was carried out about four months after deposition, in scanning transmission electron microscope high-angle annular dark field (STEM-HAADF) mode employing FEI G2 80-200 chemiSTEM in probe corrected mode with a monochromated beam. Chemical distribution of the specimen was determined with four-quadrant X-ray energy dispersive spectroscopy (XEDS) detectors. The Cliff-Lorimer factors (k-factors) were determined from binary GeTe and Sb_2Te_3 bulk targets using STEM-XEDS profiles and found to be 3.41 and 1.07 respectively. The chemical composition of the as-deposited film was measured as $\text{Ge}_{2.7}\text{Sb}_{2.2}\text{Te}_5$, with higher than expected Ge incorporation since the films were deposited by sputtering of a single $\text{Ge}_2\text{Sb}_2\text{Te}_5$ target.

Figure 1 shows a representative STEM-HAADF image of a $\text{Ge}_2\text{Sb}_2\text{Te}_5$ thin film of target thickness 30 nm deposited on a Protochips TEM fusion holder and showed an island-like morphology. The as-deposited film is comprised of isolated islands with a bimodal size distribution of average sizes ~ 15 nm and 25 nm. The space between the islands is nearly uniform and ~ 5 nm in width. The STEM-XEDS maps of Ge, Sb, and Te in as-deposited condition show

that Sb is uniformly distributed throughout the film whereas Te is concentrated within the islands and Ge is concentrated in the inter-island regions (Figure 2). XEDS analysis of the as-deposited $\text{Ge}_2\text{Sb}_2\text{Te}_5$ film shows that a significant amount of oxygen is also present (Figure 3). The peaks corresponding to Si and N can be attributed to the SiN_x membrane of the Protochips holder.

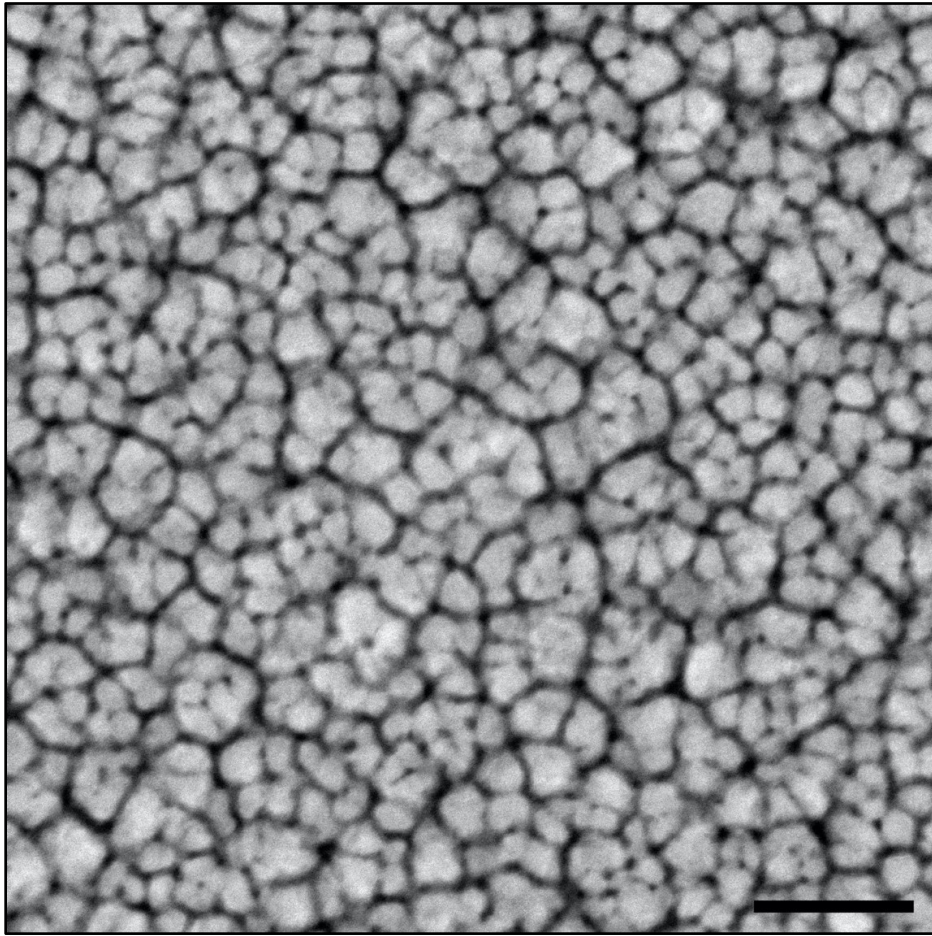


FIG. 1. Low-magnification STEM-HAADF image of $\text{Ge}_2\text{Sb}_2\text{Te}_5$ thin film of 30 nm thickness deposited by sputtering. The morphology shows the island-like nature of the as-deposited sputtered film. The scale bar is 50 nm.

The generated power spectra (FFT) of the high-resolution HAADF images acquired during in-situ heating are presented in Figure 4. The absence of lattice periodicity in the image from the as-deposited film, Figure 4(a), confirms the amorphous nature of the specimen. The power spectrum in Figure 4(b) shows the beginning of the amorphous to crystalline transformation, observed at 130 °C. The pattern could be indexed as metastable *fcc* phase of $\text{Ge}_2\text{Sb}_2\text{Te}_5$ (ICDD # 00-054-0484).

The reflections corresponding to (111) and (200) are shown in the pattern. The faint inner circle close to the direct beam may be due to the presence of untransformed clusters without any lattice periodicity. With further increase in temperature, apart from those corresponding to the fcc-hexagonal transformation (ICDD#01-082-8882), reflections corresponding to rhombohedral Sb_2Te_3 (ICDD#01-071-0393) are observed. The representative power spectrum at 200 °C is shown in Figure 4(c). The reflections (0116), (0009) correspond to the hexagonal phase and the reflections (0003), (0006) correspond to Sb_2Te_3 . The Ge-O phase is devoid of any lattice periodicity and hence doesn't provide any signature in the power spectrum. The details of this phase segregation are discussed later in the paper.

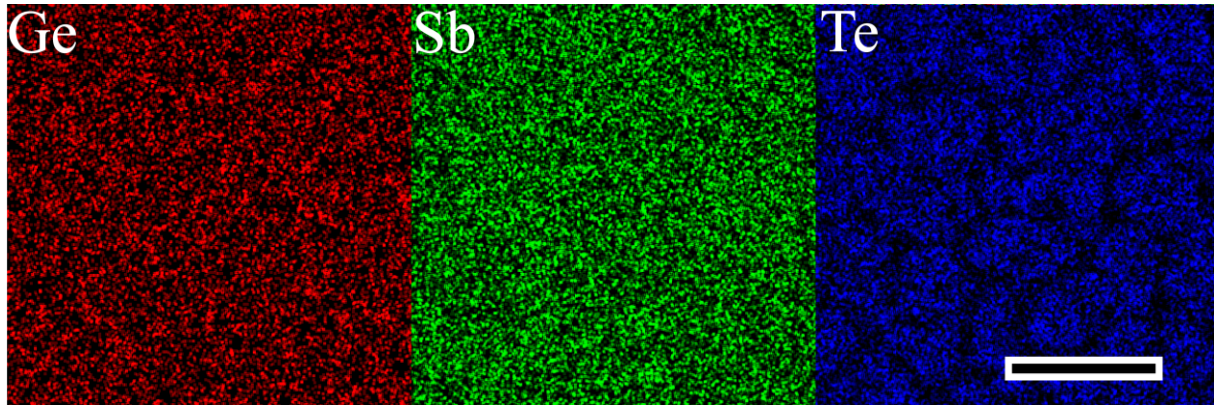


FIG.2. XEDS maps showing the distribution of Ge, Sb, and Te in the as-deposited $\text{Ge}_2\text{Sb}_2\text{Te}_5$ film. The scale bar is 50 nm.

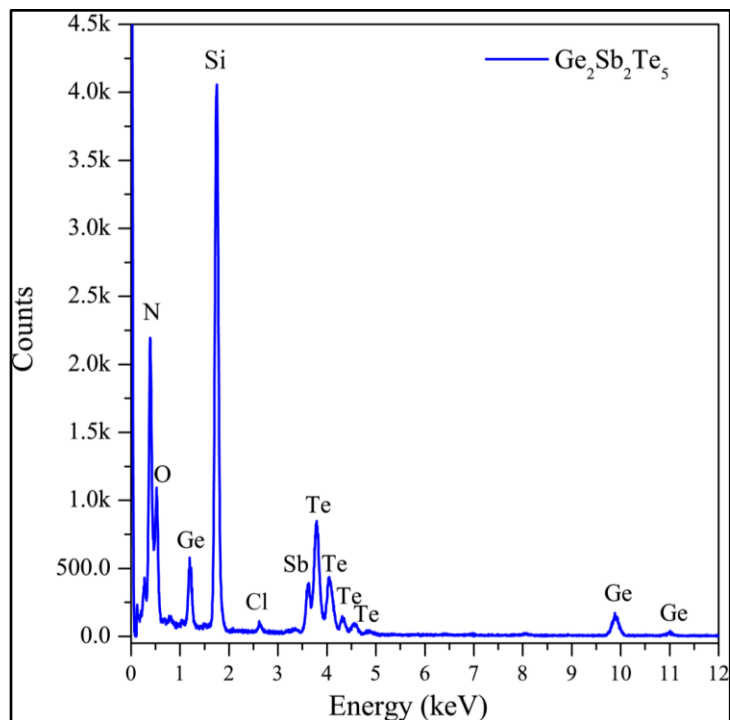


FIG. 3. X-ray energy dispersive spectrum of as-deposited 30 nm $\text{Ge}_2\text{Sb}_2\text{Te}_5$ film showing significant oxygen content.

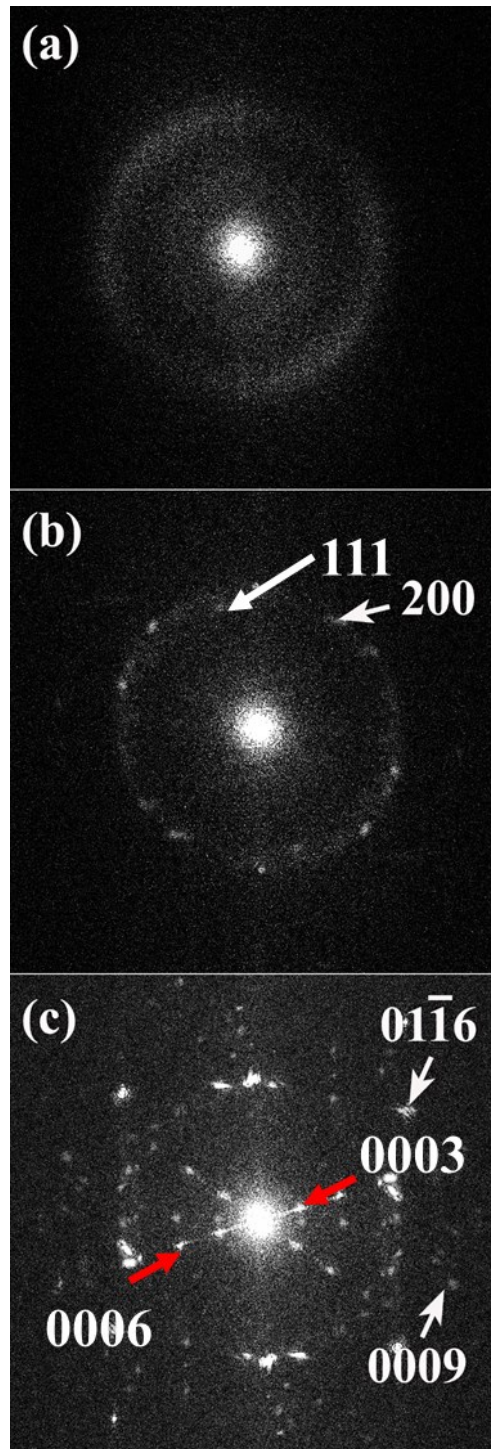


FIG. 4. Power spectrum from STEM-HAADF images of (a) as-deposited GST film at room temperature, heated at (b) 130 °C and (c) 200 °C. The phase transformation from amorphous to metastable *fcc* phase is observed at 130 °C. Figure (c) shows reflections corresponding to hexagonal $\text{Ge}_2\text{Sb}_2\text{Te}_5$ (white arrows) and rhombohedral phase of Sb_2Te_3 (red arrows).

To investigate the influence of residual oxygen during heat treatment, the composite elemental distribution map including oxygen was obtained. Figure 5 shows the XEDS profile with a composite map of Ge, Sb, Te, and O as inset from the $\text{Ge}_2\text{Sb}_2\text{Te}_5$ film in-situ treated at 200 °C inside the TEM. The XEDS profile shows that a significant amount of oxygen remained in the film after the heat treatment. The XEDS peaks corresponding to Ge and O are well separated, and their distribution in the composite map is directly interpretable. Interestingly, the distribution of oxygen has been observed in between the islands only. It is important to note that the gaps between the islands are rich in Ge and O whereas the islands are mostly composed of Sb and Te. The composite image also shows that Sb and Te are not homogeneously distributed between islands, with two distinct compositions present (shown as yellow and red islands). The Si in the profile is expected to have originated from the low-temperature deposited, silicon-rich SiN_x membrane of the Protochips holders.

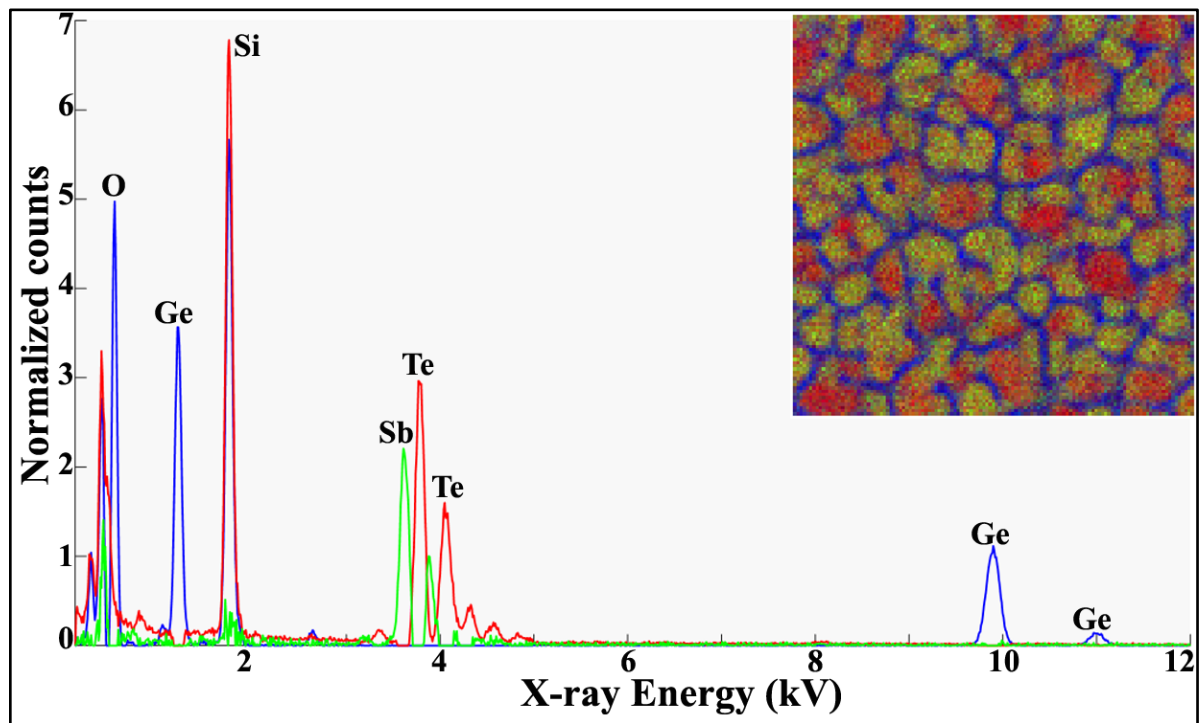


FIG. 5. XEDS profile and composite image (inset) of $\text{Ge}_2\text{Sb}_2\text{Te}_5$ including oxygen after heat treatment at 200 °C inside the TEM. The inter-island regions are enriched in Ge and O. Ge and O are shown in blue, Sb in green, and Te and Si in red, in both the map and the profile. The field of view for the composite map is 125 nm.

A series of STEM-XEDS elemental maps acquired in drift-corrected mode from the $\text{Ge}_2\text{Sb}_2\text{Te}_5$ film heated to 200 °C inside the TEM for ~1h is shown in Figure 6. The at. % concentration distribution scales associated with each of the elemental distribution maps show that the islands are almost depleted of Ge, which migrated to the gaps between the islands, whereas Sb and Te are predominantly found in the islands. This is in contrast with the XEDS map from the as-deposited film which showed Sb uniformly distributed. A composite map of all three elements is shown in Figure 6(d).

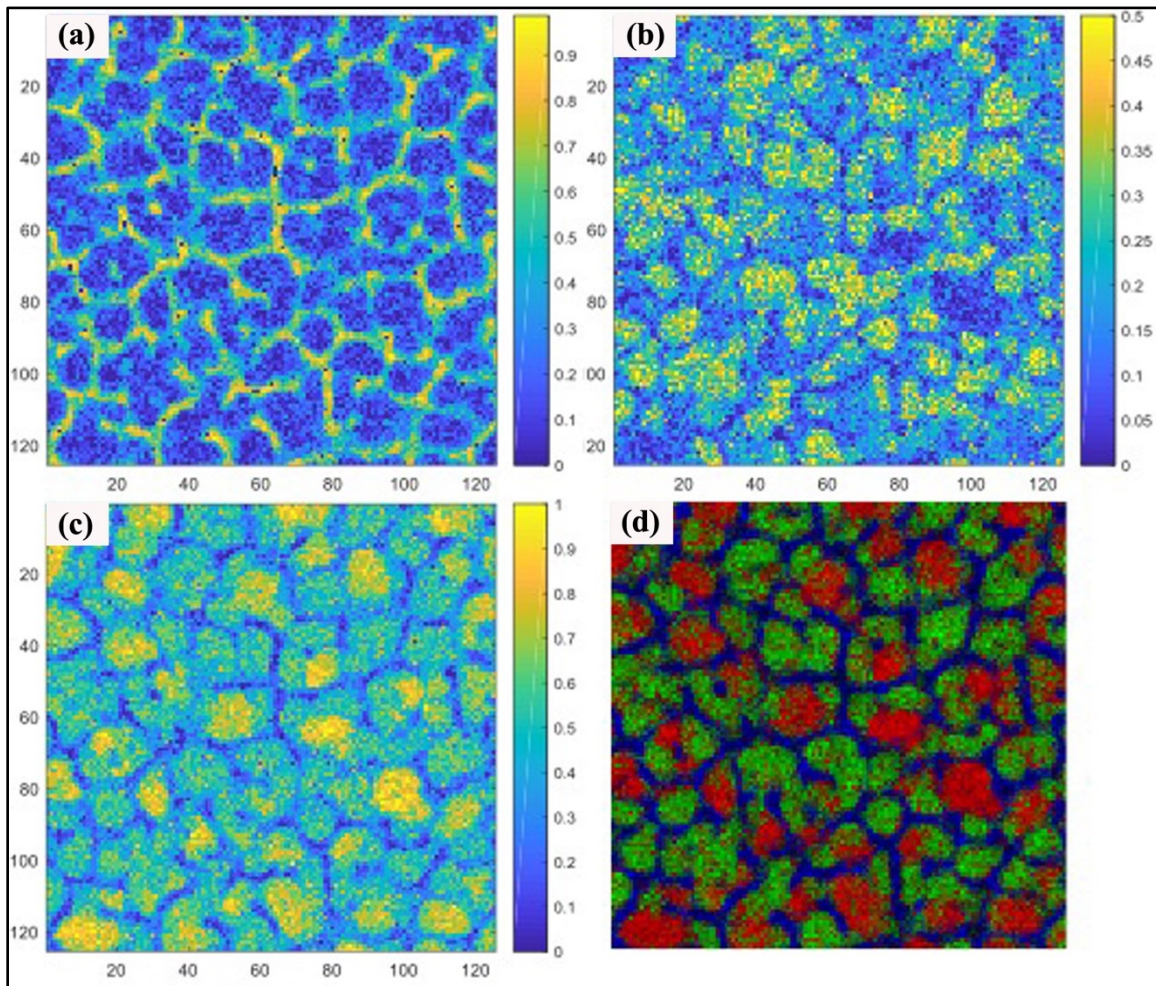


FIG. 6. STEM-HAADF chemical mapping of $\text{Ge}_2\text{Sb}_2\text{Te}_5$ thin film at room temperature after heating at 200 °C showing elemental segregation of (a) Ge, (b) Sb, and (c) Te during phase transformation. The color scale showing the concentration profile is different for each of the maps. The composite image is shown in (d) where Ge, Sb and Te are indicated in blue, green and red respectively. The field of view for all the images is 125 nm.

To quantify the chemical composition locally, STEM-XEDS elemental line profiles were acquired for the heated film. A representative STEM-HAADF image and STEM-XEDS elemental line profiles across several islands (shown as a red box) after heat treatment at 200 °C are shown in Figure 7. The morphology is similar to that of the as-deposited sample with the appearance of a band-like contrast in some of the islands. The line profiles further confirm the depletion of Ge in the islands with its redistribution in the inter-island regions and the enrichment of Sb and Te in the islands. The compositional distribution of Sb and Te along the band-like morphology regions correspond to Sb_2Te_3 composition.

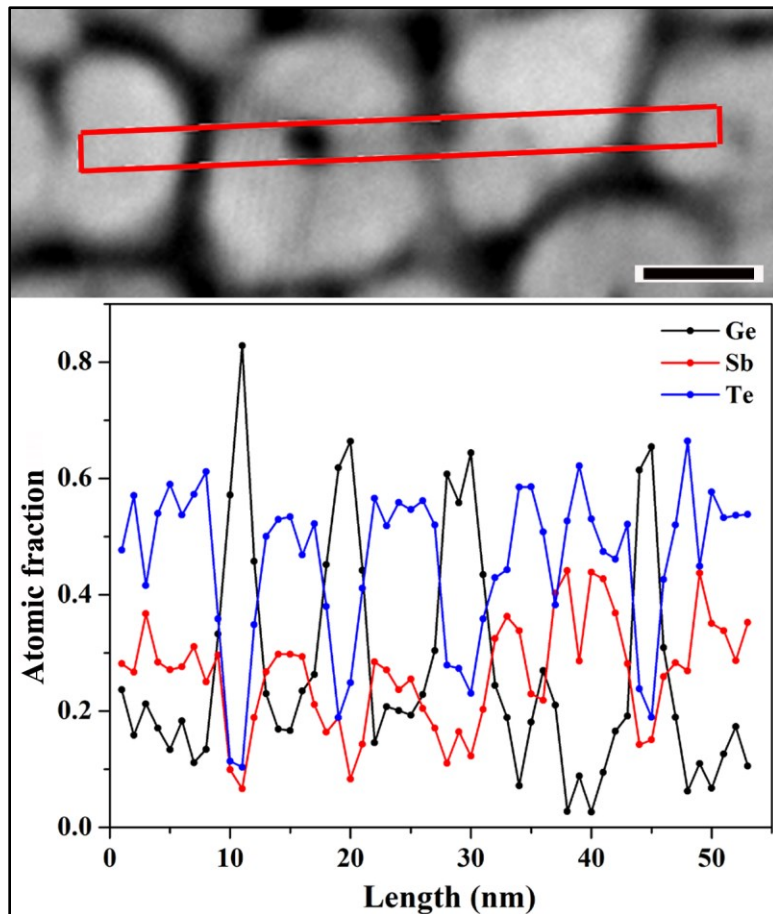


FIG. 7. STEM-HAADF image and XEDS line profiles (red box from left to right) of Ge, Sb and Te after in-situ heating at 200 °C. The scale bar for the image is 10 nm.

The accurate composition of the as-deposited and heated films is calculated from the STEM-XEDS results and determined k-factors. The absolute concentration of Ge, Sb, and Te in the as-deposited

film is determined as 0.272, 0.226, and 0.501 (at.%), corresponding to a stoichiometry of \sim $\text{Ge}_{2.7}\text{Sb}_{2.2}\text{Te}_5$. The absolute concentration of Ge, Sb, and Te in the heated film is determined as 0.297, 0.205, and 0.498 (at.%). These differences in absolute concentrations for the as-deposited and heated films are not conclusive though, as they are within the experimental detection limits. Moreover, in the heated film, both Ge-O and crystalline Sb_2Te_3 phases contribute to the concentration measurements of Ge, Sb, and Te. The chemical composition analysis does indicate higher Ge content in the as-deposited film itself, compared to that in the $\text{Ge}_2\text{Sb}_2\text{Te}_5$ sputtering target. The presence of oxygen in the inter-island regions, as shown in Figure 5, due to exposure of the uncapped film to atmosphere, further promotes the Ge segregation from the islands with the increase in temperature. The changes in elemental composition shown in Figure 6 indicate that Ge has completely migrated to the inter-island regions and combined with oxygen. A silicon-rich SiN_x membrane of the Protochips holder may have a thin SiO_2 surface layer that provided oxygen to react with Ge in the film when the temperature was increased. In the presence of excess oxygen, chemical segregation of $\text{Ge}_2\text{Sb}_2\text{Te}_5$ into Ge-O and Sb_2Te_3 is more viable than crystallization into the *fcc* and subsequent *hexagonal* phase. The bond-dissociation energy for Ge-O (657.5 kJ/mol) is much higher than that of the Ge-Te (396.7 kJ/mol), Te-O (377 kJ/mol) and Sb-O (434 kJ/mol).²³ The formation of Ge-O compound is thermodynamically more favorable than Ge remaining in the GeSbTe cluster or the formation of Sb-O or Te-O compounds. However, this situation may change when $\text{Ge}_2\text{Sb}_2\text{Te}_5$ crystalizes before exposure to oxygen. This chemical segregation occurred at a very localized level and could only be investigated with the aid of TEM. The elemental profiles in Figure 7 indicate the formation of Sb_2Te_3 in some of the islands where band contrast has been observed, in agreement with the STEM-HAADF results shown in Figure 4.

The results from this work indicate that the local chemical imbalance due to the oxidation of Ge results in a lower crystallization temperature for specific phases. Although the diffusion coefficient of Sb has been estimated to be at least 20% higher than that of Ge and Te²⁴, in the presence of oxygen, Ge diffuses out from the Ge-Sb-Te matrix. Rivera-Rodriguez and coworkers have observed the same phenomenon in the $\text{Ge}_1\text{Sb}_2\text{Te}_4$ system. They observed that in the presence of 15-28 at% of oxygen, all Ge is oxidized and Sb_2Te_3 crystallites are formed²⁵. Although Ge and Te have lower diffusion coefficients, the formation of Ge-O is thermodynamically preferred leading to the formation of amorphous Ge-O and crystalline Sb_2Te_3 phases¹⁴.

In summary, uncapped GeSbTe thin films obtained by sputtering of a $\text{Ge}_2\text{Sb}_2\text{Te}_5$ target and subsequently exposed to atmosphere consist of separate islands with an overall composition of $\sim \text{Ge}_{2.7}\text{Sb}_{2.2}\text{Te}_{5.2}$. After in-situ heating to 200 °C, the overall composition remains similar but Ge preferentially interacts with oxygen and migrates towards the inter-island regions. This chemical segregation has been confirmed through STEM-XEDS and leads to the phase separation of the uncapped $\text{Ge}_2\text{Sb}_2\text{Te}_5$ films into amorphous Ge-O boundaries and crystalline Sb-Te rich islands, with Sb_2Te_3 observed locally. These results are relevant to the design of improved $\text{Ge}_2\text{Sb}_2\text{Te}_5$ phase-change memory devices, especially to help understand the effects of any interfaces with silicon dioxide and silicon nitride on the electrical and thermal properties of the active phase-change regions.

Acknowledgments

This research is supported by NSF under award DMR-1710468. The TEM studies were carried out at CINT, an Office of Science User Facility operated for the U.S. DOE, and in the Materials Characterization Department, Sandia National Laboratories. The GST films were deposited at the Institute of Materials Science and Nanotechnology (UNAM) at Bilkent University, Turkey. The authors thank Dr. Khalid Hattar, Dr. Matthew T. Janish and Dr. Ali Gokirmak for helpful discussions. The Sandia National Laboratories are managed and operated by National Technology and Engineering Solutions of Sandia, LLC., a wholly owned subsidiary of Honeywell International, Inc., for the U.S. DOE's NNSA under contract DE-NA-0003525. The views expressed here do not necessarily represent the views of the U.S. DOE or the U.S. Government.

References

1. S. Raoux, G. W. Burr, M. J. Breitwisch, C. T. Rettner, Y.-C. Chen, R. M. Shelby, M. Salinga, D. Krebs, S.-H. Chen, H.-L. Lung, C. H. Lam, "Phase-change random access memory: a scalable technology," *IBM J. Of Res. and Devel.*, 52, 4.5 465 (2008).
2. H.-S. Philip Wong, S. Raoux, S.-B. Kim, J. Liang, J. Reifenberg, B. Rajendran, M. Asheghi, and K. E. Goodson, "Phase Change Memory," in *Proceedings of the IEEE*, 98, 12, 2201, (2010).
3. G. W. Burr, M. J. Brightsky, A. Sebastian, H.-Y. Cheng, J.-Y Wu, S. Kim, N. E. Sosa, N. Papandreou, H.-L. Lung, H. Pozidis, E. Eleftheriou, and C. H. Lam, "Recent Progress in Phase-Change Memory Technology," in *IEEE Journal on Emerging and Selected Topics in Circuits and Systems*, vol. 6, no. 2, 146 (2016).

4. J. Hegedus, S. R. Elliott, "Microscopic origin of the fast crystallization ability of Ge-Sb-Te phase-change memory materials", *Nature Materials* 7, 5, 399 (2008).
5. F. Dirisaglik, G. Bakan, Z. Jurado, S. Muneer, M. Akbulut, J. Rarey, L. Sullivan, M. Wennberg, A. King, L. Zhang, "High speed, high temperature electrical characterization of phase change materials: metastable phases, crystallization dynamics, and resistance drift", *Nanoscale* 7, 4, 16625 (2015).
6. S. Tripathi, M. Janish, F. Dirisaglik, A. Cywar, Y. Zhu, K. Jungjohann, H. Silva, C. B. Carter, "Phase-Change Materials; the Challenges for TEM," *Microscopy and Microanalysis*, 24, S1, 1904 (2018).
7. D. Lencer, M. Salinga, M. Wuttig, "Design Rules for Phase-Change Materials in Data Storage Applications," *Adv. Mater.* 23, 18, 2030 (2011).
8. M. Wuttig, N. Yamada, "Phase-change materials for rewriteable data storage" *Nature Materials*, 6, 11, 824 (2007).
9. N. Ciocchini, M. Laudato, M. Boniardi, E. Varesi, P. Fantini, A. L. Lacaita, D. Ielmini, "Bipolar switching in chalcogenide phase change memory," *Scientific Reports* 6, 29162 (2016).
10. Bin Zhang, Wei Zhang, Zhenju Shen, Yongjin Chen, Jixue Li, Shengbai Zhang, Ze Zhang, Matthias Wuttig, Riccardo Mazzarello, Evan Ma and Xiaodong Han, "Element-resolved atomic structure imaging of rocksalt Ge₂Sb₂Te₅ phase-change material," *Appl. Phys. Lett.* 108, 191902 (2016)
11. Golovchak, R., Y. G. Choi, S. Kozyukhin, Yu Chigirinsky, A. Kovalskiy, P. Xiong-Skiba, J. Trimble, R. Pafchek, and H. Jain. "Oxygen incorporation into GST phase-change memory matrix." *Applied Surface Science* 332, 533-541 (2015).
12. P.-Y. Du, J. Y. Wu, T.-H. Hsu, M.-H. Lee, T.-Y. Wang, H.-Y. Cheng, E.-K. Lai, S.-C. Lai, H.-L. Lung, S.-B. Kim, M. J. BrightSky, Y. Zhu, S. Mittal, R. Cheek, S. Raoux, E. A. Joseph, A. Schrott, J. Li, and C. Lam "The impact of melting during reset operation on the reliability of phase change memory", 2012 IEEE *Int. Reliability Physics Symposium*, 6C.2 (2012).
13. Yoon, S.-M.; Choi, K.-J.; Lee, N.-Y.; Lee, S.-Y.; Park, Y.-S.; Yu, B.-G., "Nanoscale observations of the operational failure for phase-change-type nonvolatile memory devices using Ge₂Sb₂Te₅ chalcogenide thin films," *Applied Surface Science* 254, 316 (2007).
14. M. Jang, S. Park, D. Lim, M.-H. Cho, K. Do, D.-H. Ko, H. Sohn, "Phase change behavior in oxygen-incorporated Ge₂Sb₂Te₅ films," *Applied Physics Letters* 95, 012102 (2009).

15. E. Gourvest, B. Pelissier, C. Vallée, A. Roule, S. Lhostis, S. Maitrejean, "Impact of oxidation on Ge₂Sb₂Te₅ and GeTe phase-change properties," *Journal of The Electrochemical Society* 159, H373 (2012).
16. L. Yashina, R. Püttner, V. Neudachina, T. Zyubina, V. Shtanov, M. Poygin, "X-ray photoelectron studies of clean and oxidized α -GeTe (111) surfaces," *Journal of Applied Physics*, 103, 094909 (2008).
17. Noé Pierre, Christophe Vallée, Francoise Hippert, Frédéric Fillot, and Jean-Yves Raty. "Phase-change materials for non-volatile memory devices: from technological challenges to materials science issues." *Semiconductor Science and Technology* 33, no. 1 013002 (2017).
18. Noé Pierre, Chiara Sabbione, Nicolas Bernier, Niccolo Castellani, Frédéric Fillot, and Françoise Hippert. "Impact of interfaces on scenario of crystallization of phase change materials." *Acta Materialia* 110 142 (2016).
19. B. Kooi, W. Groot, J. T. M. De Hosson, "In situ transmission electron microscopy study of the crystallization of Ge₂Sb₂Te₅," *Journal of Applied Physics* 95, 3, 924 (2004).
20. Agati, Marta, Clément Gay, Daniel Benoit, and Alain Claverie. "Effects of surface oxidation on the crystallization characteristics of Ge-rich Ge-Sb-Te alloys thin films." *Applied Surface Science* 146227 (2020).
21. Agati, Marta, François Renaud, Daniel Benoit, and Alain Claverie. "In-situ transmission electron microscopy studies of the crystallization of N-doped Ge-rich GeSbTe materials." *MRS Communications* 8(3) 1145 (2018).
22. Berthier, R., N. Bernier, D. Cooper, C. Sabbione, F. Hippert, and P. Noé. "In situ observation of the impact of surface oxidation on the crystallization mechanism of GeTe phase-change thin films by scanning transmission electron microscopy." *Journal of Applied Physics* 122(11), 115304 (2017).
23. Luo, Y.-R., *Handbook of bond dissociation energies in organic compounds*. CRC press: 2002.
24. Akola, J., and R. O. Jones. "Structural Patterns in Ge/Sb/Te Phase-Change Materials." *NIC Series* 39 169 (2008).
25. C. Rivera-Rodriguez, E. Prokhorov, G. Trapaga, E. Morales-Sanchez, M. Hernandez-Landaverde, Y. Kovalenko, J. Gonzalez-Hernandez, "Mechanism of crystallization of oxygen-doped amorphous Ge₁Sb₂Te₄ thin films," *Journal of Applied Physics* 96, 2, 1040 (2004).

